Determinants of coumarin tolerance in *Pseudomonas simiae* WCS417

Mike Bos (4602145)

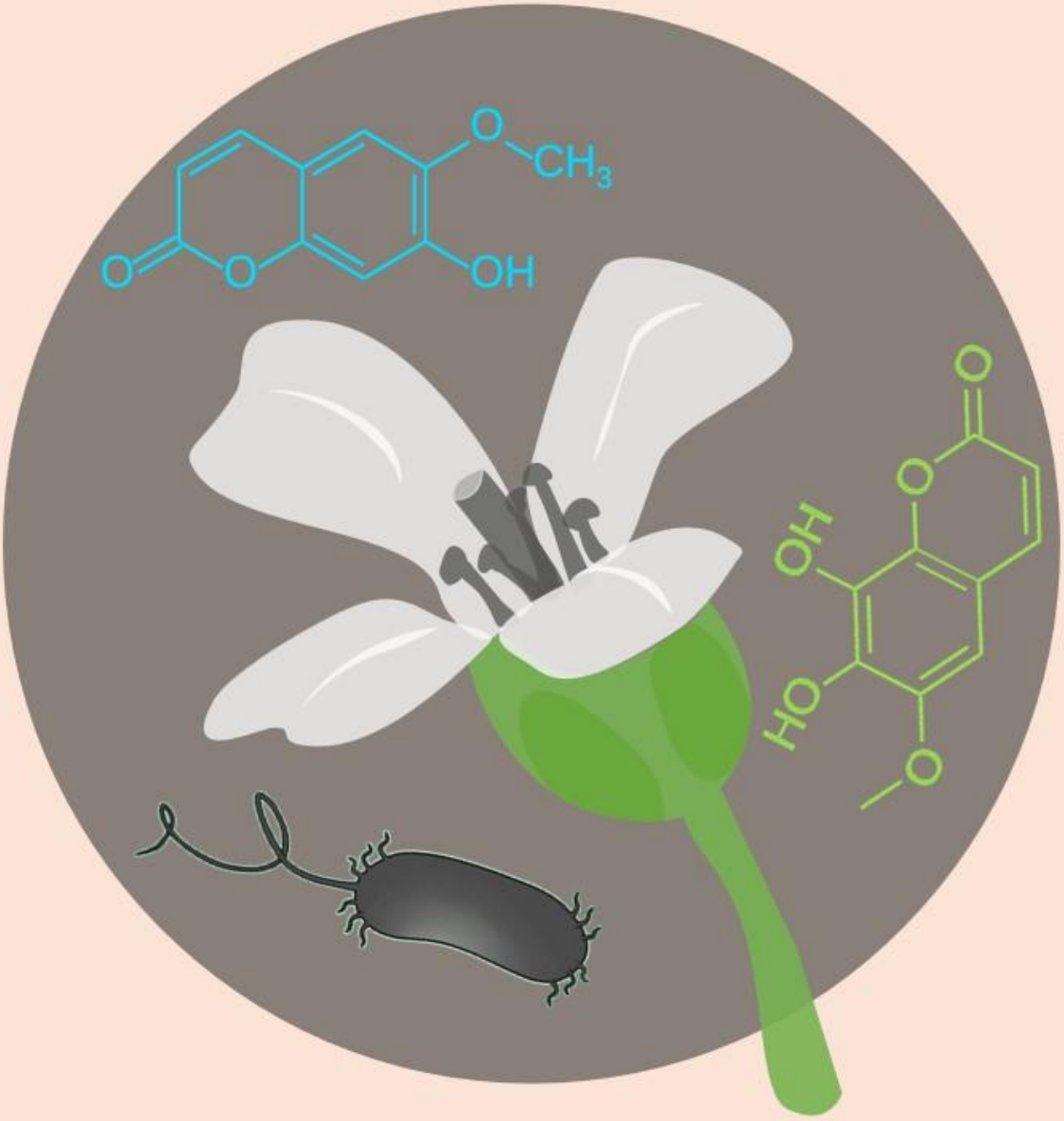

Utrecht University, Plant-Microbe Interactions
Examiner: dr. Roeland Berendsen
Daily supervisor: Max Stassen MSc
19-12-2024

Abstract

Plants are in contact with many microbes, some of which can have a positive impact, while others might have a negative impact on plant health and growth. This makes it important for plants to be able to select for microbes inhabiting their direct surroundings. The plant-root exuded coumarin scopoletin appears to be part of such a selection mechanism by differentially inhibiting bacteria and fungi. Here, a plant-growth promoting bacterium showing high tolerance to scopoletin, *Pseudomonas simiae* WCS417, is investigated for its mechanism of tolerance for scopoletin, as well as its derivative fraxetin, by screening for random mutants showing increased susceptibility. Here, several mutants with reduced tolerance are isolated, but the genetic background has not yet been investigated. Additionally, the ability of *P. simiae* WCS417 to catabolize scopoletin is shown. Moreover, an iron-dependent growth-promoting effect of fraxetin on *P. simiae* WCS417 is shown. Furthermore, a new isolation and pre-screening method using the Isolation Bio Prospector system is explored, as well as a novel method for assessing chemotaxis in plant-microbe interactions studies by using a two-layer agar system.

Layman's summary

This report explores how a plant-growth and plant-health promoting bacterium, *Pseudomonas simiae* WCS417, resists plant-produced compounds scopoletin and fraxetin, which inhibit other microbes. It is hypothesized that this tolerance allows this bacterium to thrive while harmful microbes are suppressed, aiding the plant in establishing a community of microbes with beneficial effects on their roots. To better understand the mechanism of tolerance of this bacterium, several mutant strains were tested for their growth in the presence of scopoletin and fraxetin, and some showed reduced growth. In the future, understanding the genetic basis of these mutations should help clarify this mechanism of tolerance. Additionally, experiments performed here suggest that this bacterium can break down scopoletin, whereas fraxetin seems to help it grow when iron is scarce. Gaining insight in how certain microbes are promoted or inhibited by plant-produced compounds such as scopoletin and fraxetin could have applications in agriculture, enhancing plant growth and health while reducing the need for chemical fertilizers or pesticides.

Introduction

Plants have a long history of symbioses with microorganisms, and it is believed that it was such a symbiosis that made the colonization of land possible for plants[1]. Nowadays, nearly all plants are found living together with many different microbes, with many found in area surrounding the root, otherwise known as the rhizosphere. Here, these microbes can contribute to growth and health of the plant by aiding in nutrient uptake or by improving defence against pathogens, while microbes having a negative effect may also be present[2]. Depending on the stresses a plant is exposed to, a different composition of microbes would be beneficial for its optimal health and growth. Moreover, it is of importance to be able to distinguish between friend and foe, that is between mutualists or commensals and pathogens.

A potential mechanism for microbial selection is by the secretion of exudates promoting or impeding growth of specific microbes[3]. One compound for which such an effect has been described is scopoletin, which is a coumarin[4]. In a lot of plants, including many crops, coumarins are produced from the phenylpropanoid pathway, and have been found to be produced in many species in response to pathogen infection[2,5–14]. Interestingly, the production of these compounds has also been found to be induced by iron-deficient conditions, a prevalent stress in agricultural

lands worldwide[15,16]. In these conditions, iron-deficiency pathways are induced by the transcription factor MYB72, which also controls the production of scopoletin and its derivative fraxetin[4,17]. These coumarins are involved in the uptake of Fe^{3+}, which they can reduce and chelate[18]. This mobilized form of iron can be imported via Iron-Regulated Transporter 1 (IRT1) or coumarin-iron complexes can be taken up directly via a yet unidentified mechanism[19,20]. Specifically, the presence of fraxetin, synthesized by Scopoletin 8-Hydroxylase (S8H), appeared to be of importance for alleviating an iron-stressed phenotype of model plant *Arabidopsis thaliana*[18,21].

Scopoletin on the other hand, which is synthesized via Feruloyl-CoA 6'-Hydroxylase1 (F6'H1), has been shown to have antimicrobial properties[4,5,7,8,10,11,22–25]. Moreover, the presence of scopoletin, by induction of iron stress in *f6'h1* mutant or wild type *A. thaliana*, has been found to cause a shift in the root microbiome composition[4]. Additionally, *Pseudomonas simiae* WCS417 and *P. capeferrum* WCS358, considered plant-beneficial bacteria because of their plant-growth and plant-health promoting abilities, show high tolerance to scopoletin, whereas plant-pathogenic fungi *Fusarium oxysporum* and *Verticillium dahliae* show high susceptibility[4,26]. Therefore, the presence of these *F6'H1* dependent coumarins has been hypothesized to select for and promote bacterial species that have plant-beneficial properties, possibly dependent on scopoletins antimicrobial properties. Interestingly, on top of showing high tolerance for scopoletin, *P. simiae* WCS417 appears to induce coumarin production and secretion in *A. thaliana*[18]. This way, *P. simiae* WCS417 might be able to create its own niche, where it can outcompete less tolerant species.

Multiple mechanisms for the antimicrobial effect of coumarins have been proposed. In fungi and oomycetes, this includes the inhibition of plant cell-wall degrading enzymes, spore germination and DNA and protein synthesis, as well as by causing damage to the cell membrane[28–30]. In bacteria proposed mechanisms include the suppression of type III secretion system genes and inhibition of biofilm formation and swimming motility[31–33]. In addition, coumarins appear to inhibit bacterial DNA helicase and certain efflux pumps[34,35]. However, how *P. simiae* WCS417 is able to elude the antimicrobial effect of scopoletin is not yet understood. Gaining more insight into its mechanisms of tolerance for scopoletin and fraxetin could be of interest to agriculture, as exploiting it could allow for the assembly of a plant-beneficial microbiome, promoting plant-growth and health. This could potentially reduce the need for pesticides, while improving crop yields. Therefore, the aim here is to identify genes of *P. simiae* WCS417 that improve tolerance. This is done using randomly generated mutants from a transposon insertion mutant library, which are screened for impeded growth in scopoletin and fraxetin. Potential methods of tolerance include limiting uptake, modification of targets, inactivation and efflux of these coumarins[36]. As other species of *Pseudomonas* have been found that can catabolize coumarin, inactivation of scopoletin by *P. simiae* WCS417, by catabolism, is tested by measuring the scopoletin concentration in the growth medium of *P. simiae* WCS417[37–39]. Lastly, the effects of scopoletin and fraxetin on *P. simiae* WCS417 in low iron conditions are explored in absence and presence of *A. thaliana*. Here, several candidates with reduced tolerance to scopoletin and fraxetin were found, of which the mutations are yet to be identified. Furthermore, reduction in fluorescence levels of scopoletin in the presence of *P. simiae* WCS417 are shown, indicating the catabolism of scopoletin. Lastly, improved growth of *P. simiae* WCS417 in the presence of fraxetin in low iron conditions is shown, as well as improved iron nutrition in *A. thaliana* in low iron conditions in the presence of *P. simiae* WCS417.

Results

Identification of three scopoletin sensitive mutants of selected candidates from a random mutant library

Randomly generated mutants of *P. simiae* WCS417, which were isolated from a Tn5 transposon insertion mutant library previously[40] and harboured gentamycin resistance, were tested for their sensitivity for scopoletin in a 96 well plate setup in liquid King's medium B (LKB)[41] (N = 4) (Fig. 1A). Based on initial screening performed previously[42], 136 candidates were selected (Fig. S1).

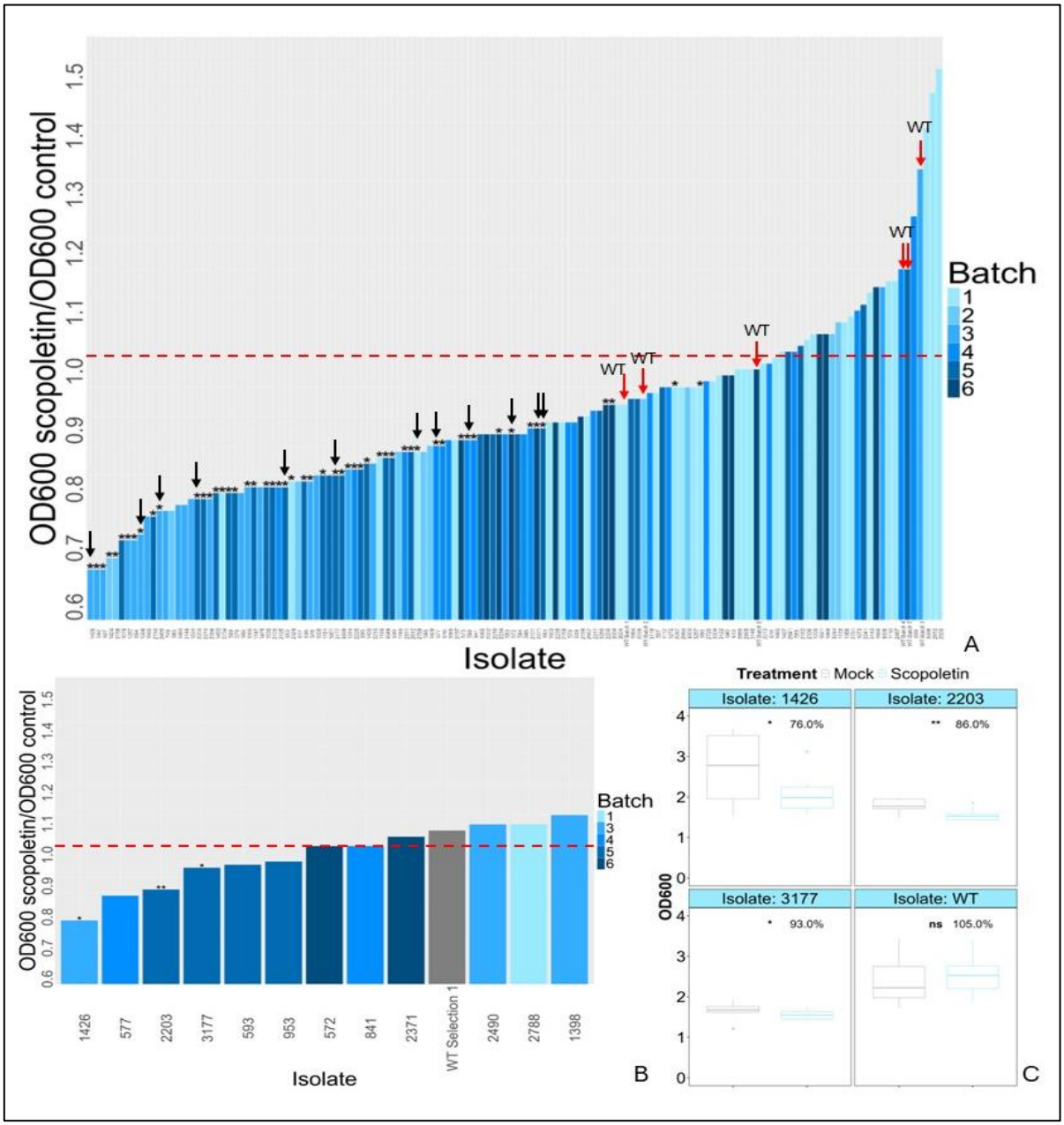

Figure 1: Screening for scopoletin sensitivity in previously isolated mutants. *(A) Growth in 2 mM scopoletin relative to control conditions of 136 best mutants selected from earlier screening tested for scopoletin tolerance (N=4). Significance level is indicated (ns, p ≥ 0.05; *, p < 0.05). Black arrows denote candidates selected for subsequent screening. Red arrows denote wild type controls. (B) Growth in 2 mM scopoletin relative to control conditions of retesting of twelve best candidates selected from previous round of screening (N=8). Significance level is indicated (ns, p ≥ 0.05; *, p < 0.05; **, p < 0.01). Black arrows denote candidates selected for subsequent screening. Red arrows denote wild type controls. (C) OD_{600} of candidate strains 1426, 2203 and 3177 and wild type* P. simiae *WCS417* in retesting round (N=8). *OD_{600} is shown for 2 mM scopoletin and mock conditions. Significance level is indicated (ns, p ≥ 0.05; *, p < 0.05; **, p < 0.01). Relative growth of 2 mM scopoletin conditions compared to control conditions is shown next to significance level.*

Best candidates were subsequently selected based on significance level ($p \leq 0.05$), effect size (≥ 10% reduced growth), and control growth compared to wild type ($p > 0.05$). The latter selection criterium was to exclude mutants with either increased growth, having a similar growth rate in the presence of scopoletin as the wild type in control conditions, or mutants with decreased growth, where the relative growth rate describes a small absolute difference. Twelve candidates were retested under the same conditions with a higher replicate count (N = 8) (Fig. 1B,C). In this rescreen, only three candidates yielded significantly reduced growth ($p \leq 0.05$), and the largest effect size was found in isolate 1426, with a growth of 76% in testing conditions compared to control conditions. However, due to high variation, and small effect size in the other remaining candidates, it was decided new candidates were to be isolated using a novel method that would potentially provide better pre-screening and initial selection.

Identification of 3 scopoletin sensitive and 4 fraxetin sensitive mutants from newly isolated candidates using the Isolation Bio Prospector system

To obtain new mutants an automatic isolation platform termed the Prospector (Isolation Bio) was utilized. It uses a nano-well setup, allowing for the isolation of single cells from the same mutant library mentioned above. Because of the use of a by NADH reducible dye, yielding a green fluorescent dye, growth could be observed by measuring red and green fluorescence per well. Similar testing and mock conditions were obtained in the Prospector array, here in Reasoner's 2 A (R2A) medium, to be used for initial selection. An initial selection was made based on the growth rate of isolates, as determined by the red/green fluorescence ratio (Fig. S2). Candidates were then isolated from the Prospector array and tested in a 96-wells plate setup under the same conditions in LKB as before (N = 4) (Fig. 2A). These isolates were also tested in R2A medium (Fig. S3). Again, a selection was made based on significance level ($p \leq 0.05$), effect size (≥ 20% reduced growth), and control growth compared to wild type ($p > 0.05$), yielding 14 best candidates, which were retested under the same testing and mock conditions as the earlier isolated candidates (N = 12) (Fig. 2B). Nine isolates were found to perform significantly worse under testing conditions compared to mock conditions ($p \leq 0.05$). All candidates from this screen were tested again, and five isolates were found to perform significantly worse in testing conditions, as well as wild type ($p \leq 0.05$, N = 12) (Fig. 2C). Only candidates ProS46, ProS57, and ProS66 were found to perform significantly worse in both testing repetitions. Next, the isolation and selection procedure using the Isolation Bio Prospector was performed again under the same conditions (Fig. S4). This selection was tested once more under the same conditions (N = 8), with two isolates performing significantly worse under testing conditions ($p \leq 0.05$) (Fig. 2D).

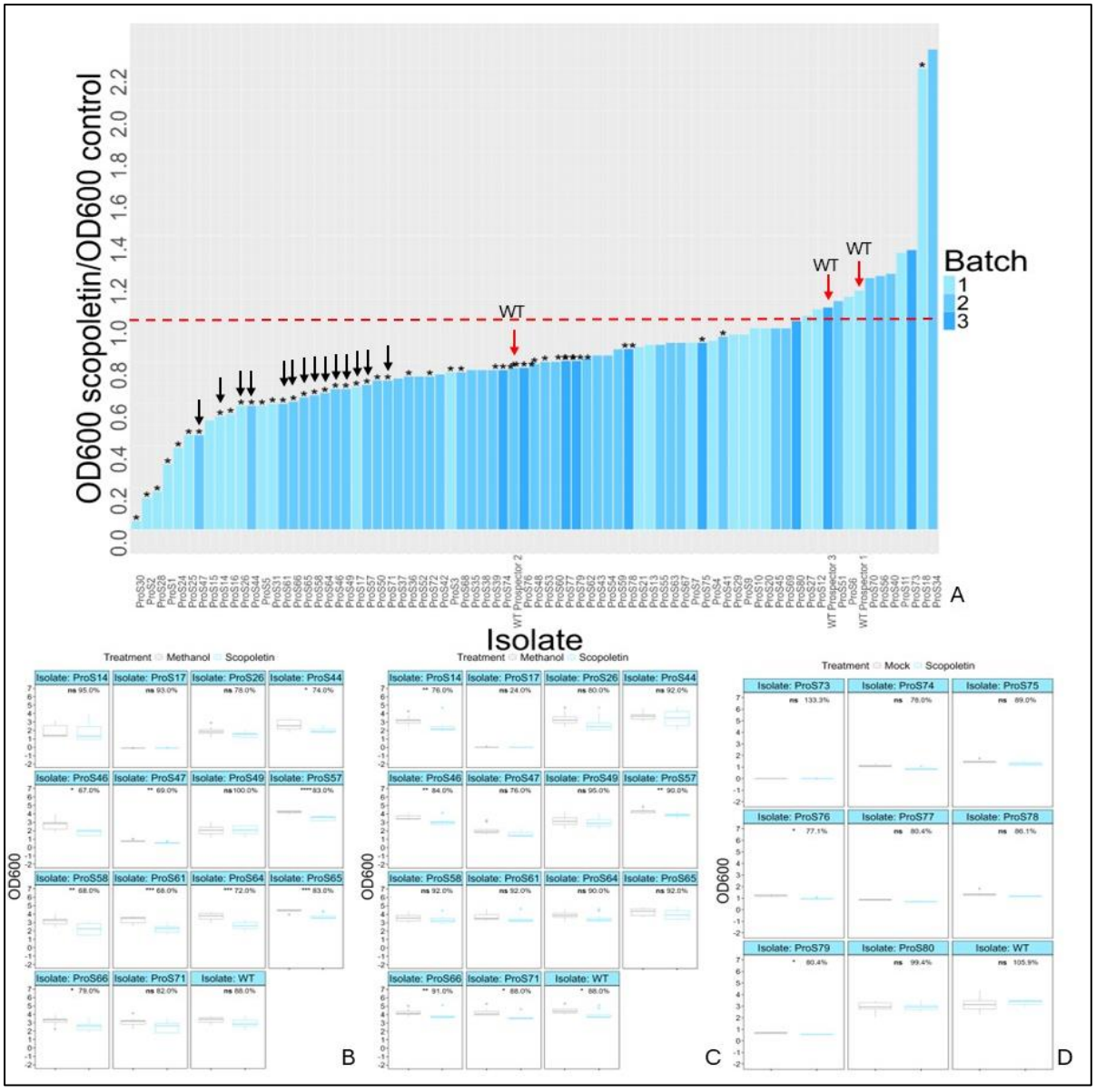

Figure 2: Screening for scopoletin sensitivity in candidates isolated using the Isolation Bio Prospector. *(A) Growth in 2 mM scopoletin relative to control conditions of 72 candidates isolated using the Isolation Bio Prospector (N=4). Significance level is indicated (ns, ≥ 0.05; *, < 0.05; **, < 0.01; ***< 0.001; ****, < 0.0001). Black arrows denote candidates selected for subsequent screening. Red arrows denote wild type controls. (B) OD_{600} of candidate strains selected from previous screen (N = 12). OD_{600} is shown for 2 mM scopoletin and mock conditions. Significance level is indicated (ns, p ≥ 0.05; *, p < 0.05; **, p < 0.01; ***, p < 0.001; ****, p < 0.0001). (C) OD_{600} of second retesting of candidate strains selected from previous screen (N = 12). OD_{600} is shown for 2 mM scopoletin and mock conditions. Significance level is indicated (ns, p ≥ 0.05; *, p < 0.05; **, p < 0.01). (D) OD_{600} of candidates of second isolation of candidate strains using the Isolation Bio Prospector (N = 8). OD_{600} is shown for 2 mM scopoletin and mock conditions. Significance level is indicated (ns, p ≥ 0.05; *, p < 0.05).*

Similarly to the previously described isolation and selection of candidates showing scopoletin sensitivity using the Isolation Bio Prospector, we aimed to identify mutants that displayed fraxetin sensitivity. Initial selection was done by observing the red/green fluorescence ratio after growing isolates in the prospector array in Reasoner's 2 A (R2A) medium supplemented with 2 mM fraxetin (Fig. S4). Selected candidates were retested in a 96 well plate setup in LKB supplemented with 2 mM fraxetin (N = 8), with 4 isolates performing significantly worse under testing conditions compared to mock conditions (Fig. 3A,B). These candidates were tested in R2A medium as well (Fig. S5).

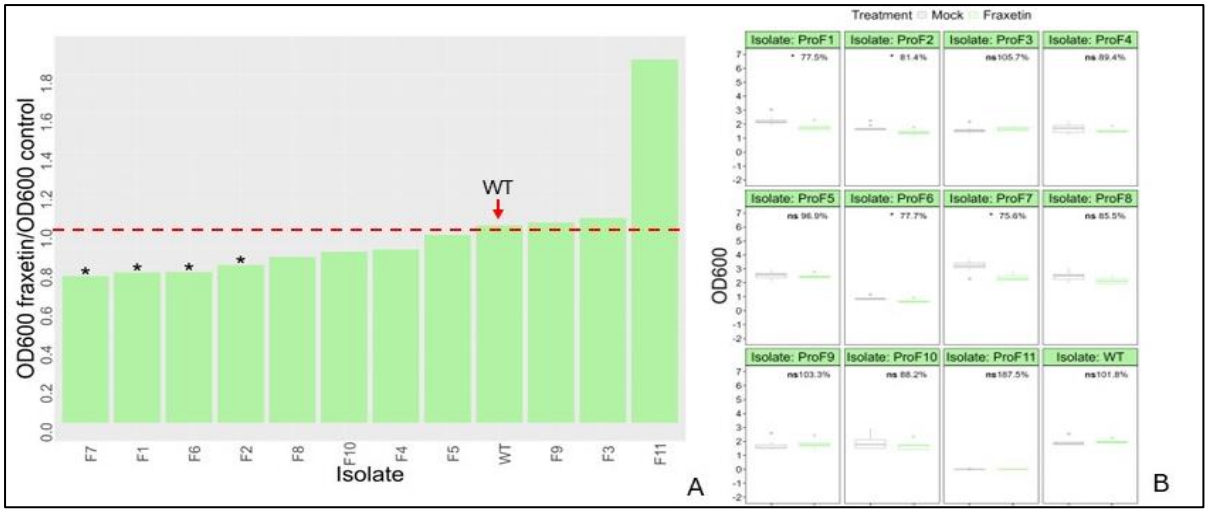

Figure 3: Screening for fraxetin sensitivity in candidates isolated using the Isolation Bio Prospector. *(A) Growth in 2 mM fraxetin relative to control conditions of 11 candidates isolated using the Isolation Bio Prospector (N=8). Significance level is indicated (ns, p ≥ 0.05; *, p < 0.05). Red arrow denotes wild type control. (B) OD_{600} of candidates isolated using the Isolation Bio Prospector. OD_{600} is shown for 2 mM fraxetin and mock conditions (N = 8). Significance level is indicated (ns, p ≥ 0.05; *, p < 0.05).*

P. simiae WCS417 decreases fluorescence of scopoletin in M9 medium

It was hypothesized that one of the potential methods of bacterial tolerance to scopoletin would be the degradation of scopoletin. To test this hypothesis, *P. simiae* WCS417 was grown in two low-nutrient media; one adapted from M9 medium[43] and one modified *Pseudomonas* specific minimal medium adapted from[37] (hereafter MM). Both were supplemented with either 100 µM scopoletin or mock conditions, and for MM 100 µM fraxetin was included as well. In M9 medium, very poor growth was observed, as depicted by low increase in OD_{600} (N = 8) (Fig. 4A). Although not significant, scopoletin appeared to inhibit growth. Additionally, no significantly larger decrease in fluorescence was observed between *P. simiae* WCS417 containing wells and *P. simiae* WCS417 non-containing wells (N = 8) (Fig.4B). In MM, better growth was observed than in M9, with no significant differences between the coumarin treatments (N = 12) (Fig. 4C). Interestingly, a significantly larger decrease in fluorescence was found between *P. simiae* WCS417 containing and *P. simiae* WCS417 non-containing wells (N = 12) (Fig. 4D).

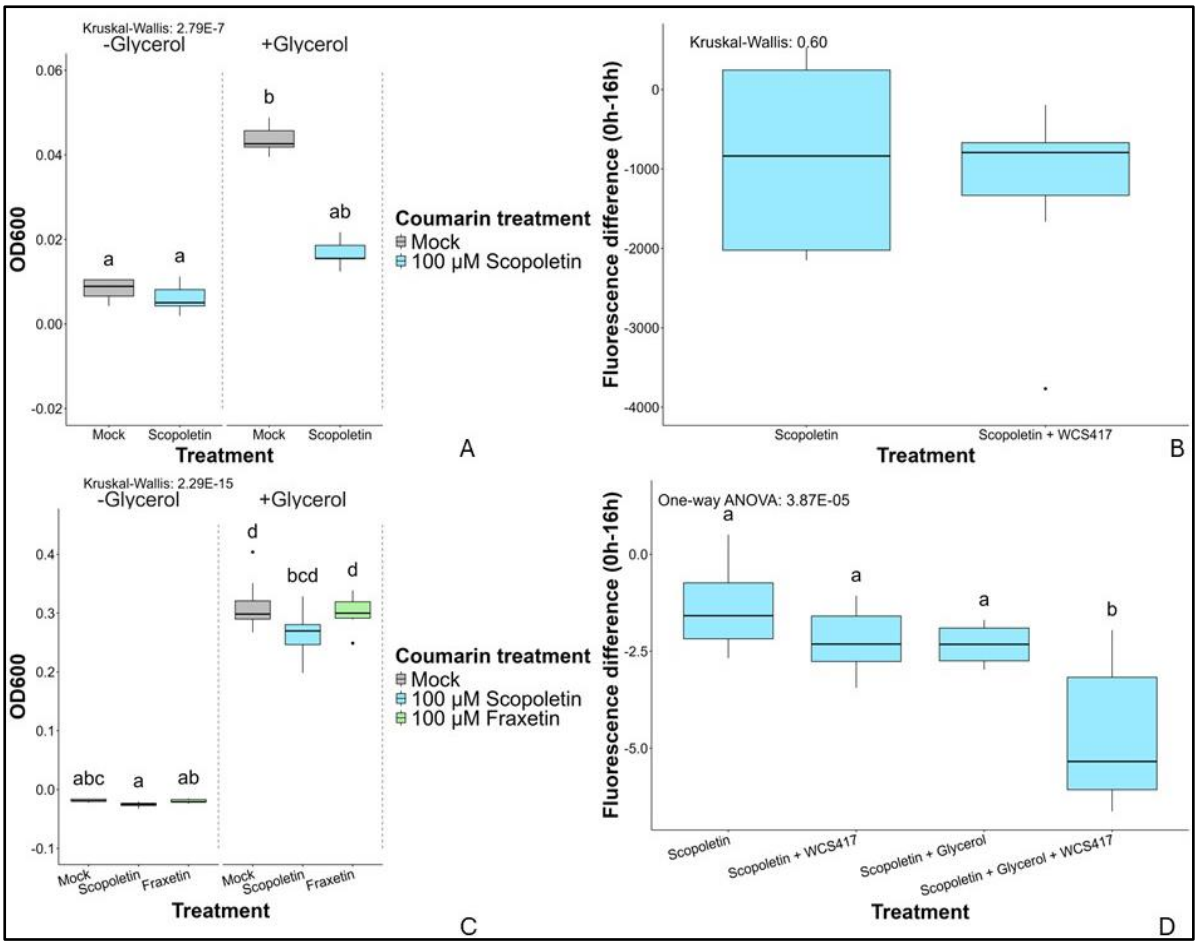

Figure 4: Growth of* P. simiae *WCS417 and scopoletin fluorescence in minimal media. *(A) OD_{600} of* P. simiae *WCS417 in M9 medium in scopoletin and mock conditions (N = 8). Different letters denote significant differences (p < 0.05). (B) Difference in fluorescence in scopoletin containing M9 medium with and without* P. simiae *WCS417 after 16 hours (N = 8). (C) OD_{600} of* P. simiae *WCS417 in MM in scopoletin, fraxetin and mock conditions (N = 12). Different letters denote significant differences (p < 0.05). (D) Difference in fluorescence in scopoletin containing MM with and without* P. simiae *WCS417 after 16 hours (N = 12).*

Fraxetin improves growth of *P. simiae* WCS417 under low-iron conditions

Because of the apparent differential effect of scopoletin on growth in M9 medium and MM, it was hypothesized that scopoletin tolerance is dependent on the iron availability, as M9 medium contains no iron source, while limited iron is present in MM. To test this, the pyoverdine mutant (*pvd*$^-$) of *Pseudomonas simiae* WCS417 was included, which lacks an iron-chelating siderophore and is less efficient in iron-uptake. MM was opted for as it allowed for better growth than M9 medium and was modified to either contain 1.1 µM Fe^{3+}-EDTA, or no source of iron. Additionally, conditions included 100 µM scopoletin, 100 µM fraxetin or mock conditions. OD_{600} was measured for both the wild type and pyoverdine mutant of *P. simiae* WCS417 and, albeit insignificant, a higher OD_{600} was found in fraxetin and Fe^{3+}-EDTA containing conditions for both genotypes compared to mock conditions (N = 14) (Fig. 5A). Next, fraxetin and mock conditions were followed over time, and during the exponential growth phase, fraxetin appeared to improve growth in Fe^{3+}-EDTA containing conditions (N = 10) (Fig. 5B). The areas under the curve only differed significantly between -Fe and 1.1 µM Fe-EDTA conditions in wild type *P. simiae* WCS417, indicating that iron nutrition is important for growth, while again improved growth in fraxetin conditions compared to mock conditions appears to be present (Fig.5C). Although not significantly, a similar trend of increased OD_{600} in fraxetin and Fe^{3+}-EDTA containing conditions was observed at 20 hours (Fig. 5D).

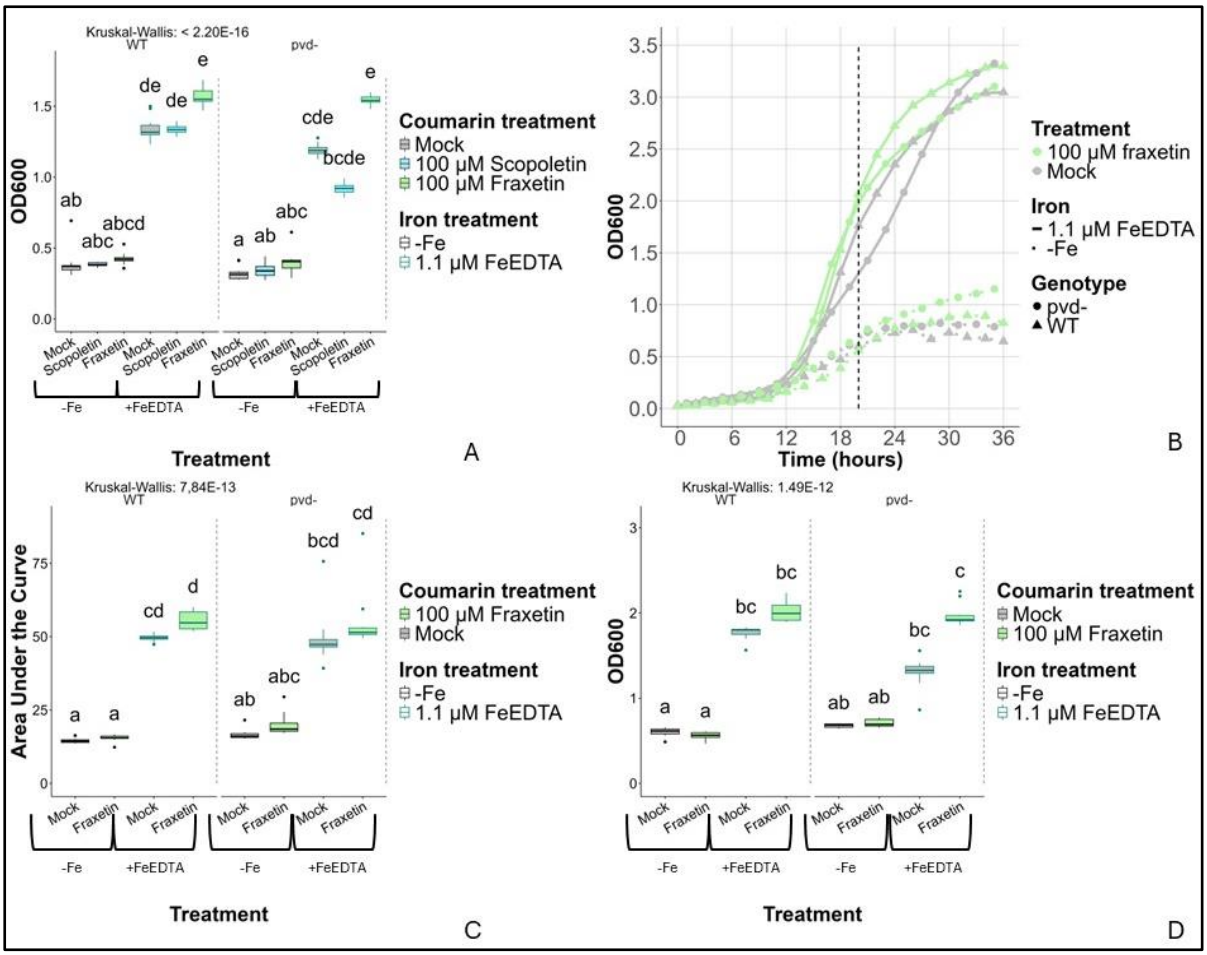

Figure 5: Growth of* P. simiae *WCS417 wild type and* pvd⁻ *in MM. *(A) OD_{600} of* P. simiae *WCS417 wild type and* pvd⁻ *grown in MM in scopoletin, fraxetin and mock conditions with or without Fe^{3+}-EDTA (N = 14). Different letters denote significant differences ($p < 0.05$). (B) Average OD_{600} of* P. simiae *WCS417 wild type and* pvd⁻ *grown in MM in fraxetin and mock conditions with or without Fe^{3+}-EDTA over 36 hours (N = 10). (C) Areas under the curve of* P. simiae *WCS417 wild type and* pvd⁻ *grown in MM in fraxetin and mock conditions with or without Fe^{3+}-EDTA followed over 36 hours (N=20). Different letters denote significant differences ($p < 0.05$). (D) OD_{600} of* P. simiae *WCS417 wild type and* pvd⁻ *grown in MM in fraxetin and mock conditions with or without Fe^{3+}-EDTA at 20 hours (N = 10). Different letters denote significant differences ($p < 0.05$).*

A. thaliana chlorophyll content is affected by fraxetin and pyoverdine presence

Fraxetin appears to improve iron nutrition of *P. simiae* WCS417 *in vitro*. Therefore, a similar effect in the presence of *A. thaliana* would be expected. To test this, *P. simiae* WCS417 wild type and *pvd⁻* strains were added to the plant-growth medium where *A. thaliana* strains Col-0 and fraxetin biosynthesis mutant *s8h-1* were transplanted. Roots, shoots and agar samples were collected to test for several growth and nutrition markers. Firstly, shoot fresh weight was significantly higher in *s8h-1* compared to wild type in *P. simiae* WCS417 wild type and mock treatments (N = 25) (Fig. 6A). No significant differences were observed between different treatments for either genotype, except between *pvd⁻* and mock treatment in the *s8h-1* genotype. Secondly, no significant differences in root fresh weight were observed (N = 5) (Fig. 6B). Lastly, chlorophyll content was found to be significantly lower for either plant genotype upon *P. simiae* WCS417 *pvd⁻* treatment (N = 25) (Fig. 6C). Unfortunately, due to contamination issues, no bacterial colony counts could be performed.

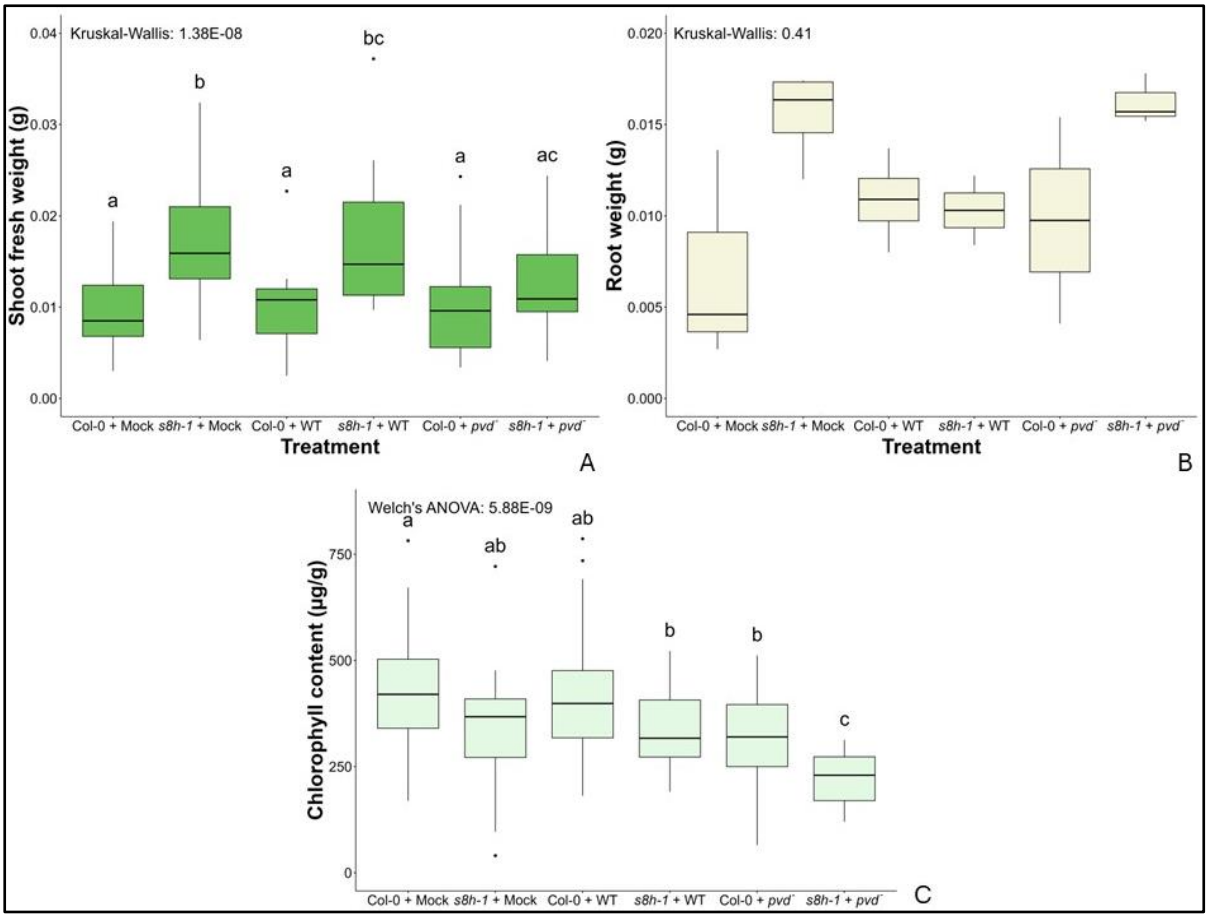

Figure 6: Plant shoot weight, root weight, and chlorophyll content after* P. simiae *WCS417 treatment. *(A) Shoot fresh weight of* A. thaliana *Col-0 and* s8h-1 *genotypes upon* P. simiae *WCS417 wild type,* pvd⁻*, or mock treatment (N = 25). Different letters denote significant differences ($p < 0.05$). (B) Root fresh weight of* A. thaliana *Col-0 and* s8h-1 *genotypes upon* P. simiae *WCS417 wild type,* pvd⁻*, or mock treatment (N = 5). Different letters denote significant differences ($p < 0.05$). (C) Chlorophyll content of shoots of* A. thaliana *Col-0 and* s8h-1 *genotypes upon* P. simiae *WCS417 wild type,* pvd⁻*, or mock treatment (N = 25). Different letters denote significant differences ($p < 0.05$).*

This experiment was repeated under slightly different conditions (see Methods). No significant difference was observed in shoot dry weight and shoot fresh weight (N = 5) (Fig. 7A,B). Higher root fresh weight was observed in Col-0 when treated with *P. simiae* WCS417 *pvd*⁻ compared to wild type *P. simiae* WCS417 (N = 15) (Fig. 7C). Contrarily, in the *s8h-1* genotype, lower root weight was observed in *P. simiae* WCS417 *pvd*⁻ treated plants compared to *P. simiae* WCS417 wild type treated plants. Next, albeit insignificant, lower total iron content was observed in both plant genotypes upon *P. simiae* WCS417 *pvd*⁻ treatment compared to *P. simiae* WCS417 *pvd*⁻ treatment (N = 5) (Fig. 7D). Lastly, bacterial colony counts were performed on root and agar samples (N =15) (Fig. 7E). Surprisingly, for most samples, low counts of or no colonies were observed for most treatments, with only one sample containing *P. simiae* WCS417 *pvd*⁻ colonies.

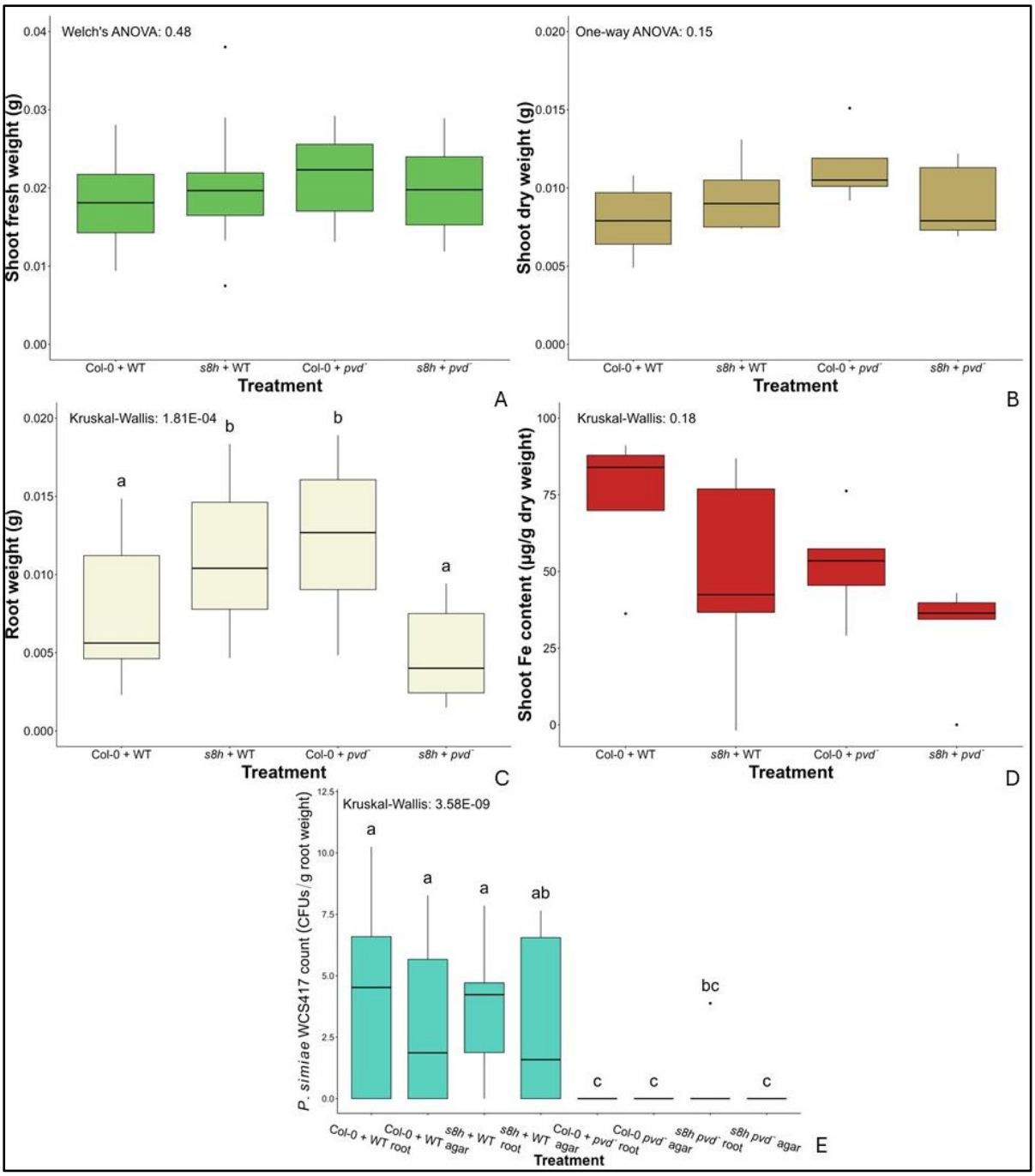

Figure 7: Plant shoot weight, root weight, iron content and bacterial colonization after* P. simiae *WCS417 treatment. *(A) Shoot fresh weight of* A. thaliana *Col-0 and* s8h-1 *genotypes upon* P. simiae *WCS417 wild type or* pvd⁻ *treatment (N = 5). (B) Shoot dry weight of* A. thaliana *Col-0 and* s8h-1 *genotypes upon* P. simiae *WCS417 wild type or* pvd⁻ *treatment (N = 5). (C) Root fresh weight of* A. thaliana *Col-0 and* s8h-1 *genotypes upon* P. simiae *WCS417 wild type or* pvd⁻ *(N = 15). Different letters denote significant differences (p < 0.05). (D) Iron content of shoots of* A. thaliana *Col-0 and* s8h-1 *genotypes upon* P. simiae *WCS417 wild type,* pvd⁻*, or mock treatment (N = 5). (E) Colonization of* P. simiae *WCS417 wild type and* pvd⁻ *genotypes on root and agar samples of* A. thaliana *Col-0 and* s8h *-1(N = 15). Different letters denote significant differences (p < 0.05).*

A novel method for testing *in vitro* plant root exudate-dependent bacterial chemotaxis reveals potential flagellar-independent root colonization of *P. simiae* WCS417

To test attraction and colonization of bacteria mediated by plant root-exudates, a two-layer agar system was developed by Hsu (see Methods). Using this setup, *P. simiae* WCS417 wild type and flagella lacking mutant Mob10[44] were added to the bottom layer of agar, with either *A. thaliana* Col-0 or scopoletin biosynthesis mutant *f6'h1* transplanted on the agar. Root, shoot and top layer agar samples were collected to assess mobility and colonization (N = 20). Interestingly, *P. simiae* WCS417 Mob10 was found in all sample types (Fig. 8), indicating a flagellar-independent movement towards the plant. In all treatments, a pattern arises, with roots having the highest bacterial colony counts, followed by shoots and agar. No significant differences were observed between plant or bacterial genotypes, indicating no flagellar-dependent motility inducing properties of *F6'H1*-dependent exudates on *P. simiae* WCS417.

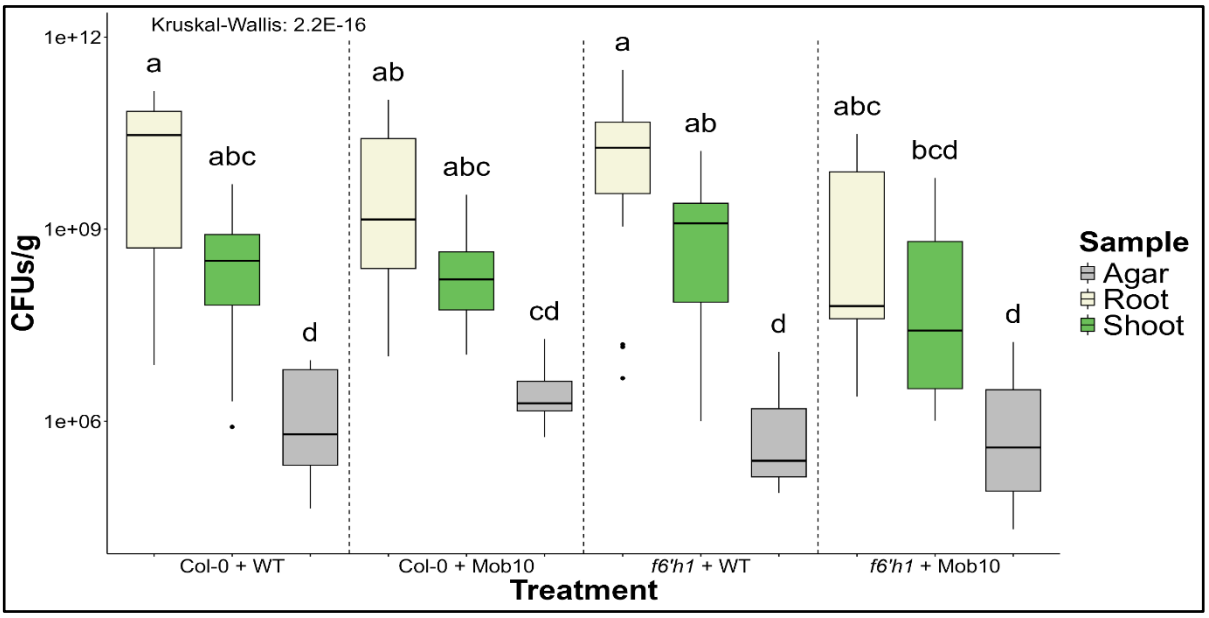

Figure 8:* P. simiae *WCS417 wild type and flagella-lacking mutant Mob10 colony forming unit (CFU) counts on* A. thaliana *wild type and* f6'h1 *genotype roots, shoots and top-layer agar. P. simiae *WCS417 wild type and Mob10 mutant CFU counts when grown in bottom-agar layer of a two-layer agar system with* A. thaliana *wild type and* f6'h1 *grown on the top layer (N=20). Different letters denote significant differences ($p < 0.05$).*

Discussion

Here, 6 randomly generated mutants of *P. simiae* WCS417, isolated from a transposon insertion mutant library with decreased tolerance for scopoletin, as well as 4 with a decreased tolerance for fraxetin have been identified. The cause of this decreased tolerance, however, is yet unknown. Therefore, these candidates will be sent for sequencing, to unravel the molecular and genetic background of its tolerance to these coumarins. The location of the transposon insertion can be found with a two-step PCR approach using primers binding the known sequence of the transposon, as well as arbitrary primers, a technique known as arbitrarily primed PCR[45]. Mutations in genes in pathways involved in, among other things, efflux pumps, catabolism of coumarins, as well as targets of scopoletin and fraxetin would be expected to be found. However, before sequencing, this cannot be confirmed.

Interestingly, the Prospector preselection approach yielded a higher portion of candidates after subsequent rounds of testing, indicating a potentially more efficient preselection compared to a colony picking approach. In the colony picking approach the preselection might be less efficient due to these tests containing only single replicates of unknown cell densities, making this setup more variable than the Prospector approach, where each nano-well supposedly contains a single cell[46]. Depending on the costs of the growth medium, this Prospector approach could prove a cost-effective method as well. A major downside, however, is an increased contamination risk during the transfer to a multi-well plate, as the Prospector itself does not provide a sterile environment. Although the isolates here harboured gentamycin resistance, not all candidates could be saved. Another downside is that no distinction can be made between low growth due to a decrease in coumarin tolerance or because of another mutation causing reduced growth in the Prospector, however in subsequent testing this distinction can be made, and isolates growing poorly in control conditions can be filtered.

To investigate the possibility of scopoletin tolerance by catabolism in *P. simiae* WCS417, scopoletin concentration was measured using fluorescence in a minimal medium setup with and without the presence of glycerol as a carbon source. A reduction in fluorescence of scopoletin when added in the growth medium of *P. simiae* WCS417 was found. This reduction is significantly less when no bacteria are added. Although it should be considered that the presence of *P. simiae* WCS417 can disturb these fluorescence measurements, as the cells might absorb some of the light and the pyoverdine secreted by this bacterium is fluorescent as well, it appears scopoletin is catabolized by *P. simiae* WCS417[26]. This could be a way of tolerance for scopoletin. However, for more certainty, a more accurate approach should be used for quantifying scopoletin, such as high-performance liquid chromatography. In addition, similar to experiments described above, a random mutant screening approach could be used to deduce the genetic background of this phenomenon, which would give further insight in the molecular mechanism involved. Additionally, as *P. simiae* WCS417 did not grow well in the absence of glycerol with either scopoletin or fraxetin supplementation, it appears these compounds are not used as a carbon source by this bacterium.

Moreover, an increased growth rate of *P. simiae* WCS417 was observed in the presence of fraxetin in low-iron conditions. This effect was also seen in the *pvd*$^{-}$ strain of *P. simiae* WCS417, which is a synthesis mutant of the iron-chelating siderophore pyoverdine produced by this bacterium[26]. In addition to this, because this effect is not observed in the absence of iron, and because of the iron binding properties of fraxetin, it appears that this increased growth rate is due to altered iron nutrition. Interestingly, in a … comparative genomics study investigating scopoletin and fraxetin tolerance amongst *Pseudomonads*, genes annotated to be involved in iron acquisition were found to be related to fraxetin tolerance in *Pseudomonas* spp (Stassen *et al.*, unpublished). Therefore, it is hypothesized here that *P. simiae* WCS417 can use fraxetin-bound iron, improving its growth in low-iron conditions. Interestingly, this increased growth rate was observed for *Pseudomonas synxantha* and *Pseudomonas aeruginosa* in similar conditions in an earlier study as well[47]. This could be a mechanism of microbial selection as well, as microbes with the ability to use this fraxetin-bound iron would be promoted in low-iron conditions, whereas microbes that do not possess this ability would be impeded in their growth. This effect should be further explored, with different species of bacteria tested for their growth in low-iron conditions in the presence and absence of fraxetin. Additionally, the mechanism behind this effect should be investigated. Therefore, *P. simiae* WCS417 mutants with decreased tolerance for fraxetin should be tested in this setup. With knowledge of the genes involved, the molecular mechanism can be discovered.

To investigate if the same effect is present in the presence of plants, *P. simiae* WCS417 wild type and its pyoverdine mutant were added to plant medium harbouring low-iron conditions. Here, markers of iron nutrition, chlorophyll and total Fe-content, were decreased in *A. thaliana* upon *P. simiae* WCS417 *pvd*$^{-}$ treatment. Seemingly, pyoverdine is important for a reducing an iron-stressed phenotype in *A. thaliana*, which has been observed before[48,49]. Although fraxetin appears to improve growth of *P. simiae* WCS417 *in vitro* in the plant medium assay, unexpectedly low colony counts were observed. Therefore, to determine the importance of pyoverdine and fraxetin for *A. thaliana* root colonization by *P. simiae* WCS417, these experiments should be repeated. Similarly, different bacterial species, as well as mutants with decreased fraxetin tolerance should be tested in this setup to explore this interaction further.

Lastly, a new method for plant root exudate-dependent bacterial chemotaxis was tested using *A. thaliana* wild type and scopoletin biosynthesis mutant *f6'h1*, and *P. simiae* WCS417 wild type and flagellar mutant Mob10. Here, a preference for growth of *P. simiae* WCS417 on the root of *A. thaliana* over shoot and agar was observed. This phenomenon has been observed before and was deemed the rhizosphere effect[3]. Unexpectedly, *P. simiae* WCS417 Mob10 was still able to colonize roots and shoots and the top agar layer equally efficient as the wild type. Apparently, this movement and colonization happens independent of flagella. In an earlier study, a downregulation of genes involved in motility, specifically flagellar biosynthesis, in *P. simiae* WCS417 in response to F6'H1 dependent root exudates was found[44]. Therefore, a flagellar-independent mechanism of root-colonization is hypothesized. Pseudomonads posses several forms of motility, including swimming and swarming motility, which are both flagellar-dependent[50,51]. Alternatively, pseudomonads possess the ability of moving by twitching, which is instead dependent on type IV pili[51]. Similarly, sliding motility has also been observed in pseudomonads, which is independent of both flagella and type IV pili and instead arises from the division of cells[50,52]. As *P. simiae* WCS417 possesses the genes required for type IV pilus assembly, neither twitching nor sliding motility can be excluded[26]. To determine the form of motility that led to the observed movement of *P. simiae* WCS417 Mob10, a double mutant, lacking both flagella and type IV pili, should be created and tested in the same setup.

Methods

Mutant library isolation with the prospector

A *P. simiae* WCS417 Tn5 transposon insertion mutant library[40] -80 °C stock, containing an estimated $19.5 \cdot 10^9$ CFUs·mL^{-1} as determined by colony counting, was thawed at room temperature, after which it was diluted in Reasoner's 2 A (R2A) medium, containing either 2 mM scopoletin or 3.2% methanol, to an estimated 200.000 bacteria per mL. Next, 1.5 mL 200 µM Prospector Dye Reagent in R2A medium was added to 1.5 mL of the diluted mutant library. The Prospector Dye Reagent is a dye fluorescent upon excitation with red light, and can be reduced by NADH, yielding a dye fluorescent upon excitation with green light[46]. Because of its responsiveness to NADH, the red/green fluorescence ratio can be used as an indicator for cell growth. Subsequently, the suspension was loaded onto the Prospector array according to the manufacturers instructions[46]. The array was sealed and incubated at 20°C, and red and green fluorescence was measured regularly. Based on the red and green fluorescence intensity, wells were selected for transfer to Greiner CELLSTAR clear flat bottom 96 well plate wells containing R2A medium containing 50 µg·mL^{-1} gentamicin. The 96 well plate was incubated at 28 °C for 2

days, after which the content of the wells were transferred to 1.5 mL tubes and 25% glycerol was added. Tubes were stored at -80 °C.

For a second iteration, 2 mM fraxetin was included as a condition in a prospector array. After growth, selected isolates from the prospector array were transferred to clear F-bottom 96 well plate wells containing R2A medium with, depending on the array of origin, either 2 mM scopoletin or 2 mM fraxetin, as well as to R2A medium containing 3.2% methanol. Due to contaminations, isolates were moved to wells containing R2A medium with 50 $\mu g \cdot mL^{-1}$ gentamicin using sterile inoculation loops. Content of wells selected based on visible contaminations were transferred to Eppendorf tubes and 25% glycerol was added. Tubes were stored at -80 °C.

Bacterial growth conditions

For different assays, *P. simiae* WCS417, *P. simiae* WCS417 *pvd*$^-$, and *P. simiae* WCS417 mutants isolated from a transposon insertion mutant library (Goossens, unpublished) were used. Bacteria were added from glycerol stocks kept at -80 °C to 15 mL falcon tubes containing 7 mL liquid King's medium B (LKB)[41]. The tubes were kept overnight in a shaking incubator at 28 °C and 150 RPM. Before use in each assay, bacteria were washed by centrifuging the bacteria-containing 15 mL tubes at 4500 g, after which supernatant was discarded and 10 mM $MgSO_4$ was added to reach a final volume of 7 mL, which was subsequently vortexed for 5 minutes at 2000 RPM, repeating this twice.

Plant material and growth conditions

Seeds of *A. thaliana* accessions Col-0 and *s8h-1*[18] were sterilised in a desiccator in chlorine gas for 3 hours. Next, they were sown on 1× Murashige and Skoog (MS) medium (1% agar, pH 5.7) supplemented with 0.5% sucrose. For the stratification process, seed-containing plates were stored in the dark at 4 °C for 48 hours, after which they were moved to a growth chamber (22°C; 10 h light/14 h dark; light intensity 100 µmol·m−2 ·s −1), placed upright.

Tolerance assays

OD_{600} was measured using a spectrophotometer, after which bacteria were diluted in LKB to an estimated OD_{600} of 0.02 in a 1.5 mL tube, and vortexed briefly. Next, 100 µL was transferred to clear F-bottom 96 well plate wells containing 100 µL LKB with 4 mM scopoletin or fraxetin, previously dissolved in 80% methanol 50 mM stock solution, or a mock treatment of eight percent 80% methanol. Final concentrations were 3.2% methanol, with either 2 mM scopoletin, fraxetin or no additional compounds, with a final estimated OD_{600} of 0.01 (except for blanks, where no bacteria were added), in LKB. 96-wells plates were incubated in the dark at 28°C for approximately 16-18 hours, after which plates were shaken for 5 seconds and OD_{600} was measured using a BioTek Synergy H1 microplate reader. OD_{600} results obtained from the microplate reader were corrected to better correspond to 1 cm pathlength spectrophotometer measurements by multiplying by 3.21, which was determined by comparing OD_{600} measurements between the spectrophotometer and the microplate reader (Figure S6).

Scopoletin degradation and bacterial growth assays

OD_{600} was measured using a spectrophotometer, after which bacteria were diluted in 10 mM $MgSO_4$ to an estimated OD_{600} of 0.1 in a 1.5 mL tube, and vortexed briefly. Next, depending on the assay, bacteria were diluted in adapted M9 medium or adapted minimal medium (MM), with or without 10 $g \cdot L^{-1}$ glycerol replacing glucose a carbon source, containing 0.16% methanol and either 100 µM scopoletin, fraxetin, or no additional compound, to a final estimated OD_{600} of 0.01.

MM would contain either 1.1 µM $FeSO_4$, Fe^{3+}-EDTA, or $FeCl_3$, or no added Fe source. After brief vortexing, 200 µL of the suspension was moved to clear F-bottom 96 well plate wells for OD_{600} measurements, and to Greiner CELLSTAR black flat bottom 96 well plate wells for fluorescence measurements and incubated in the dark at 28 °C for approximately 16-18 hours. After incubation, OD_{600} was measured using a microplate reader and results were corrected to better correspond to 1 cm pathlength spectrophotometer measurements by multiplying by 3.10. Scopoletin degradation was determined by measuring fluorescence emission at 438 nm after excitation at 336 nm. For determining the growth curve, a single 96 well plate was incubated in the dark at 20 °C in the microplate reader, measuring OD_{600} every 30 minutes.

Plant root colonization, plant weight measurements and iron-nutrition assessments

OD_{600} was measured using a spectrophotometer, after which bacteria were diluted in 10 mM $MgSO_4$ to an estimated OD_{600} of 0.1 in an Eppendorf tube, and vortexed briefly. Bacteria were diluted 1000 times in Hoagland medium (0,5% sucrose, 0.7% agar, pH 7.3). For mock conditions, a corresponding volume of 10 mM $MgSO_4$ was added to the medium. After solidification in 50 mL square Petri dishes, five ten-day old seedlings (*A. thaliana* Col-0 and *s8h-1*) per plate were transferred onto this medium and kept in a growth chamber (22 °C; 10 h light/14 h dark; light intensity 100 µmol·m−2 ·s −1) in upright position for seven days (Fig. S7). Then, the 17-day old plants were harvested, with roots cut from the shoots. Roots were taken together per plate, while shoots were harvested separately. Fresh weight was determined by weighing roots and shoots, and 1 mL 100% acetone was added to shoots, which were subsequently incubated at 28 °C and 150 RPM overnight. Acetone solution was transferred to cuvettes and absorbance was measured at 662 nm and at 645 nm using a spectrophotometer. Chlorophyll content was determined using the formula A662 × 7.05 + A645 × 18.09 and was expressed as µg per g shoot fresh weight.

For a second iteration, Hoagland medium without sucrose was used and shoots were harvested together per plate, as well as agar samples. Additionally, no mock bacterial condition was included. Plates containing no plants were included. No chlorophyll measurements were performed. Shoot samples were dried at 60 °C for 6 days in open 15 mL falcon tubes. Next, 225 µL 65% nitric acid was added and tubes were incubated at 95 °C for 6 hours, being vortexed briefly every 90 minutes. Then, 150 µL hydrogen peroxide was added and tubes were incubated at 56 °C for 2 hours, being vortexed every 60 minutes, after which 225 µL Milli-Q was added. Tubes were stored overnight in the dark at 4 °C. The next day, a 5 µL sample of the digested plant material was added to clear F-bottom 96 well plate wells, after which 245 µL assay solution (1 mM bathophenanthrolinedisulfonic acid disodium salt hydrate, 0.6 M sodium acetate and 0.48 M hydroxylamine hydrochloride in Milli-Q) was added. Next, absorbance at 535 nm was measured. Iron content was determined by plotting included standard solutions containing known Fe^{3+} concentrations, which yielded the formula: Fe content = 50.22 * A535. Total iron content was expressed as µg per g shoot dry weight.

One millilitre 50% glycerol in sterile Milli-Q was added to agar samples and root samples, which were then grinded using the Qiagen Tissuelyser II at 30 Hertz for 2 minutes. Samples were stored at -20 °C for 7 days, after which a dilution series was made by diluting the sample 10 times in sterile Milli-Q, and repeating 7 times (10^0-10^8 dilution factors) with the newly obtained dilution. The dilution series was plated on King's medium B containing 50 µg L^{-1} rifampicin and incubated in the dark at 28 °C overnight. Next, the amount of colony forming units (CFUs) were determined for each sample, counting the dilution with 5 - 20 colonies where possible. Counted colonies were multiplied by the corresponding dilution factor and corrected to 1 mL. CFUs were expressed as CFUs per g fresh root weight or per g agar.

Two-layer agar chemotaxis and colonization experiment

Hoagland medium (0.5% sucrose, 0.7% agar, pH 5.5) was supplemented with either 10^5 CFU mL^{-1} *P. simiae* WCS417 wild type or *P. simiae* WCS417 Mob10, of which 25 mL was added to a square Petri dish. After solidification, 25 mL Hoagland medium (0.5% sucrose, 0.7% agar, pH 5.5) was added on top of this layer. Five ten-day old *A. thaliana* Col-0 and *f6'h1* plants per plate were transplanted onto this medium (Fig. S8). Plates were stored in a growth chamber (22 °C; 10 h light/14 h dark; light intensity 100 µmol·m−2 ·s −1) in upright position for seven days. Then, 17-day old plants were harvested, roots were cut from shoots, and both were weighed with all plants per plate collected in an Eppendorf tube. Additionally, agar samples from the top agar layer were collected and weighed. 1 mL of 10 mM $MgsSO_4$ was added to each sample. Samples were grinded using the Qiagen Tissuelyser II, and dilution series was made using 10 mM $MgSO_4$ to obtain dilution factors 10^0-10^8. 5 µL sample was plated on King's medium B containing 50 µg L^{-1} rifampicin, with 2 replicates per sample. Plates were stored at 28 °C overnight, after which CFUs were counted. Counts were multiplying by dilution factor and corrected to 1 mL, and results were expressed as CFUs per g.

Microplate reader pathlength corrections

To more intuitively quantify results obtained with the microplate reader, a method for pathlength correction to 1 cm was investigated. This was done by making a dilution series to get suspensions of *P. simiae* WCS417 in LKB, R2A, and 10 mM $MgSO_4$, with estimated OD_{600} ranging from 0.008 to 2.5. The OD_{600} of all samples in these dilution series were then measured using both the spectrophotometer, which has a pathlength of 1 cm, and the microplate reader. Measurements were plotted and tested for a linear relationship using the Pearson correlation coefficient. All tests yielded a strong ($r > 0.99$) and statistically significant ($p < 0.05$) correlation. A linear regression model was fitted to the data, and the slope was used to find the multiplication factor for pathlength correction (Figure S6). Due to the y-intercept being very small, this was assumed 0. This led to the conclusion that for correcting the OD_{600} as measured by the microplate reader to a 1 cm path length, this result should be multiplied by 3.21 for LKB, 3.31 for R2A, and 3.10 $MgSO_4$. For minimal medium experiments, the multiplication factor for $MgSO_4$ was used for pathlength correction.

Statistical analysis

To determine the proper tests to use, data was tested for normality and homogeneity of variance. Normality was assessed using the Shapiro-Wilk test. When normality could reasonably be assumed ($p \geq 0.05$), the Levene's test was used to assess homogeneity of variance. In this case, when homogeneity of variance could reasonably be assumed ($p \geq 0.05$), a One-way ANOVA would be used for mean comparison between three or more groups, with a Tukey-HSD post-hoc test. If homogeneity of variance could not be assumed, a Welch's ANOVA would be performed instead, using a Games-Howell post-hoc test. If normality could not be assumed, A Kruskal-Wallis test with a Dunn's post-hoc test would be used. For all tolerance assays, only comparing two groups, Mann-Whitney U tests were performed. These tests were one-sided, as to only investigate reduced OD_{600} values.

References

1. Pirozynski KA, Malloch DW. The origin of land plants: A matter of mycotrophism. *Biosystems*. 1975;6(3):153-164. doi:10.1016/0303-2647(75)90023-4

2. Stringlis IA, de Jonge R, Pieterse CMJ. The age of coumarins in plant–microbe interactions. *Plant Cell Physiol*. 2019;60(7):1405-1419. doi:10.1093/pcp/pcz076

3. Sasse J, Martinoia E, Northen T. Feed your friends: do plant exudates shape the root microbiome? *Trends in Plant Science*. 2018;23(1):25-41. doi:10.1016/j.tplants.2017.09.003

4. Stringlis IA, Yu K, Feussner K, et al. MYB72-dependent coumarin exudation shapes root microbiome assembly to promote plant health. *Proc Natl Acad Sci U S A*. 2018;115(22):E5213-E5222. doi:10.1073/pnas.1722335115

5. Churngchow N, Rattarasarn M. Biosynthesis of scopoletin in Hevea brasiliensis leaves inoculated with Phytophthora palmivora. *Journal of Plant Physiology*. 2001;158(7):875-882. doi:10.1078/0176-1617-00230

6. El Oirdi M, Trapani A, Bouarab K. The nature of tobacco resistance against Botrytis cinerea depends on the infection structures of the pathogen. *Environmental Microbiology*. 2010;12(1):239-253. doi:10.1111/j.1462-2920.2009.02063.x

7. Garcia D, Sanier C, Macheix JJ, D'Auzac J. Accumulation of scopoletin in Hevea brasiliensis infected by Microcyclus ulei (P. Henn.) V. ARX and evaluation of its fungitoxicity for three leaf pathogens of rubber tree. *Physiological and Molecular Plant Pathology*. 1995;47(4):213-223. doi:10.1006/pmpp.1995.1053

8. Goy PA, Signer H, Reist R, et al. Accumulation of scopoletin is associated with the high disease resistance of the hybrid Nicotiana glutinosa × Nicotiana debneyi. *Planta*. 1993;191(2):200-206.

9. Prats E, Bazzalo ME, León A, Jorrín JV. Fungitoxic effect of scopolin and related coumarins on Sclerotinia sclerotiorum. A way to overcome sunflower head rot. *Euphytica*. 2006;147(3):451-460. doi:10.1007/s10681-005-9045-8

10. Sun H, Wang L, Zhang B, et al. Scopoletin is a phytoalexin against Alternaria alternata in wild tobacco dependent on jasmonate signalling. *J Exp Bot*. 2014;65(15):4305-4315. doi:10.1093/jxb/eru203

11. Valle T, López JL, Hernández JM, Corchete P. Antifungal activity of scopoletin and its differential accumulation in Ulmus pumila and Ulmus campestris cell suspension cultures infected with Ophiostoma ulmi spores. *Plant Science*. 1997;125(1):97-101. doi:10.1016/S0168-9452(97)00057-5

12. Gnonlonfin GJB, Sanni A, Brimer L. Review scopoletin – a coumarin phytoalexin with medicinal properties. *Critical Reviews in Plant Sciences*. 2012;31(1):47-56. doi:10.1080/07352689.2011.616039

13. Lončar M, Jakovljević M, Šubarić D, et al. Coumarins in food and methods of their determination. *Foods*. 2020;9(5):645. doi:10.3390/foods9050645

14. Antika LD, Tasfiyati AN, Hikmat H, Septama AW. Scopoletin: a review of its source, biosynthesis, methods of extraction, and pharmacological activities. *Zeitschrift für Naturforschung C*. 2022;77(7-8):303-316. doi:10.1515/znc-2021-0193

15. Schmid NB, Giehl RFH, Döll S, et al. Feruloyl-CoA 6'-hydroxylase1-dependent coumarins mediate iron acquisition from alkaline substrates in Arabidopsis. *Plant Physiol*. 2014;164(1):160-172. doi:10.1104/pp.113.228544

16. Takahashi M, Nakanishi H, Kawasaki S, Nishizawa NK, Mori S. Enhanced tolerance of rice to low iron availability in alkaline soils using barley nicotianamine aminotransferase genes. *Nat Biotechnol*. 2001;19(5):466-469. doi:10.1038/88143

17. Paffrath V, Tandron Moya YA, Weber G, von Wirén N, Giehl RFH. A major role of coumarin-dependent ferric iron reduction in strategy I-type iron acquisition in Arabidopsis. *The Plant Cell*. 2024;36(3):642-664. doi:10.1093/plcell/koad279

18. Rajniak J, Giehl RFH, Chang E, Murgia I, von Wirén N, Sattely ES. Biosynthesis of redox-active metabolites in response to iron deficiency in plants. *Nat Chem Biol*. 2018;14(5):442-450. doi:10.1038/s41589-018-0019-2

19. Eide D, Broderius M, Fett J, Guerinot ML. A novel iron-regulated metal transporter from plants identified by functional expression in yeast. *Proc Natl Acad Sci U S A*. 1996;93(11):5624-5628.

20. Robe K, Stassen M, Chamieh J, et al. Uptake of Fe-fraxetin complexes, an IRT1 independent strategy for iron acquisition in Arabidopsis thaliana. Published online August 4, 2021. doi:10.1101/2021.08.03.454955

21. Siwinska J, Siatkowska K, Olry A, et al. Scopoletin 8-hydroxylase: a novel enzyme involved in coumarin biosynthesis and iron-deficiency responses in Arabidopsis. *J Exp Bot*. 2018;69(7):1735-1748. doi:10.1093/jxb/ery005

22. El Modafar C, Clerivet A, Fleuriet A, Macheix JJ. Inoculation of Platanus acerifolia with Ceratocystis fimbriata F. Sp. Platani induces scopoletin and umbelliferone accumulation. *Phytochemistry*. 1993;34(5):1271-1276. doi:10.1016/0031-9422(91)80014-R

23. Silva WPK, Deraniyagala SA, Wijesundera RLC, Karunanayake EH, Priyanka UMS. Isolation of scopoletin from leaves of Hevea brasiliensis and the effect of scopoletin on pathogens of H. brasiliensis. *Mycopathologia*. 2002;153(4):199-202. doi:10.1023/a:1014910132595

24. Breton F, Sanier C, d'Auzac J. Scopoletin production and degradation in relation to resistance of Hevea brasiliensis to Corynespora cassiicola. *Journal of Plant Physiology*. 1997;151(5):595-602. doi:10.1016/S0176-1617(97)80236-2

25. Carpinella MC, Ferrayoli CG, Palacios SM. Antifungal synergistic effect of scopoletin, a hydroxycoumarin isolated from melia azedarach L. fruits. *J Agric Food Chem*. 2005;53(8):2922-2927. doi:10.1021/jf0482461

26. Pieterse CMJ, Berendsen RL, de Jonge R, et al. Pseudomonas simiae WCS417: star track of a model beneficial rhizobacterium. *Plant Soil*. 2021;461(1):245-263. doi:10.1007/s11104-020-04786-9

27. Zamioudis C, Hanson J, Pieterse CMJ. β-Glucosidase BGLU42 is a MYB72-dependent key regulator of rhizobacteria-induced systemic resistance and modulates iron deficiency responses in Arabidopsis roots. *New Phytol*. 2014;204(2):368-379. doi:10.1111/nph.12980

28. Rastija V, Vrandečić K, Ćosić J, et al. Effects of coumarinyl Schiff bases against phytopathogenic fungi, the soil-beneficial bacteria and entomopathogenic nematodes: deeper insight into the mechanism of action. *Molecules*. 2022;27(7):2196. doi:10.3390/molecules27072196

29. Chen YZ, Wang SR, Li T, Zhang GC, Yang J. Antifungal activity of 6-methylcoumarin against Valsa mali and its possible mechanism of action. *Journal of Fungi*. 2023;9(1):5. doi:10.3390/jof9010005

30. Wang B, Li P, Xu S, et al. Inhibitory effects of the natural product esculetin on Phytophthora capsici and its possible mechanism. *Plant Disease*. 2021;105(6):1814-1822. doi:10.1094/PDIS-09-20-2054-RE

31. Yang L, Ding W, Xu Y, et al. New insights into the antibacterial activity of hydroxycoumarins against Ralstonia solanacearum. *Molecules*. 2016;21(4):468. doi:10.3390/molecules21040468

32. Yang L, Guan D, Valls M, Ding W. Sustainable natural bioresources in crop protection: antimicrobial hydroxycoumarins induce membrane depolarization-associated changes in the transcriptome of Ralstonia solanacearum. *Pest Management Science*. 2021;77(11):5170-5185. doi:10.1002/ps.6557

33. Yang L, Li S, Qin X, et al. Exposure to umbelliferone reduces Ralstonia solanacearum biofilm formation, transcription of type III secretion system regulators and effectors and virulence on tobacco. *Frontiers in Microbiology*. 2017;8. Accessed July 4, 2023. https://www.frontiersin.org/articles/10.3389/fmicb.2017.01234

34. Li B, Pai R, Di M, et al. Coumarin-based inhibitors of Bacillus anthracis and Staphylococcus aureus replicative DNA helicase: chemical optimization, biological evaluation, and antibacterial activities. *J Med Chem*. 2012;55(24):10896-10908. doi:10.1021/jm300922h

35. Roy SK, Kumari N, Pahwa S, et al. NorA efflux pump inhibitory activity of coumarins from Mesua ferrea. *Fitoterapia*. 2013;90:140-150. doi:10.1016/j.fitote.2013.07.015

36. Reygaert WC. An overview of the antimicrobial resistance mechanisms of bacteria. *AIMS Microbiol*. 2018;4(3):482-501. doi:10.3934/microbiol.2018.3.482

37. Gu Y, Li T, Yin CF, Zhou NY. Elucidation of the coumarin degradation by *Pseudomonas* sp. strain NyZ480. *Journal of Hazardous Materials*. 2023;457:131802. doi:10.1016/j.jhazmat.2023.131802

38. Zhao Z, Liu C, Xu Q, et al. Pathway for biodegrading coumarin by a newly isolated Pseudomonas sp. USTB-Z. *World J Microbiol Biotechnol*. 2021;37(5):89. doi:10.1007/s11274-021-03055-w

39. Huang S, Wang M, Mao D, et al. Isolation, identification and characterization of growth parameters of Pseudomonas putida HSM-C2 with coumarin-degrading bacteria. *Molecules*. 2022;27(18):6007. doi:10.3390/molecules27186007

40. Goossens P. The generation of a Pseudomonas mutant library to investigate rhizosphere fitness traits. Published online Unpublished.

41. King EO, Ward MK, Raney DE. Two simple media for the demonstration of pyocyanin and fluorescin. *J Lab Clin Med*. 1954;44(2):301-307.

42. Chavan E. Identification of WCS417 coumarin resistance mutants. Published online Unpublished.

43. M9 minimal medium (standard). *Cold Spring Harb Protoc*. 2010;2010(8):pdb.rec12295. doi:10.1101/pdb.rec12295

44. Yu K, Stringlis IA, Bentum S van, et al. Transcriptome signatures in Pseudomonas simiae WCS417 shed light on role of root-secreted coumarins in Arabidopsis-mutualist communication. *Microorganisms*. 2021;9(3):575. doi:10.3390/microorganisms9030575

45. Das S, Noe JC, Paik S, Kitten T. An improved arbitrary primed PCR method for rapid characterization of transposon insertion sites. *Journal of Microbiological Methods*. 2005;63(1):89-94. doi:10.1016/j.mimet.2005.02.011

46. Prospector® System User Guide. Published online 2022. https://isolationbio.com/resource/prospector-system/

47. McRose DL, Li J, Newman DK. The chemical ecology of coumarins and phenazines affects iron acquisition by pseudomonads. *Proceedings of the National Academy of Sciences*. 2023;120(14):e2217951120. doi:10.1073/pnas.2217951120

48. Trapet P, Avoscan L, Klinguer A, et al. The Pseudomonas fluorescens siderophore pyoverdine weakens Arabidopsis thaliana defense in favor of growth in iron-deficient conditions. *Plant Physiology*. 2016;171(1):675-693. doi:10.1104/pp.15.01537

49. Truong HN, Fournier C, Hichami S, et al. Apo-siderophores promote growth of iron-deficient *Arabidopsis* plants by mobilizing iron from roots to shoots and reducing oxidative stress in roots. *Plant Stress*. 2024;12:100488. doi:10.1016/j.stress.2024.100488

50. Zegadło K, Gieroń M, Żarnowiec P, et al. Bacterial motility and its role in skin and wound infections. *Int J Mol Sci*. 2023;24(2):1707. doi:10.3390/ijms24021707

51. Sampedro I, Parales RE, Krell T, Hill JE. Pseudomonas chemotaxis. *FEMS Microbiology Reviews*. 2015;39(1):17-46. doi:10.1111/1574-6976.12081

52. Murray TS, Kazmierczak BI. Pseudomonas aeruginosa exhibits sliding motility in the absence of type IV pili and flagella. *Journal of Bacteriology*. 2008;190(8):2700-2708. doi:10.1128/jb.01620-07

Declaration of Generative AI and AI-assisted technologies in the writing process

During the writing of this report, ChatGPT (OpenAI, GPT-4) was used to assist with generating R code for the design of figures, specifically for their visual appearance. The content and interpretation of the data in the figures were not influenced by AI assistance.

Supplemental

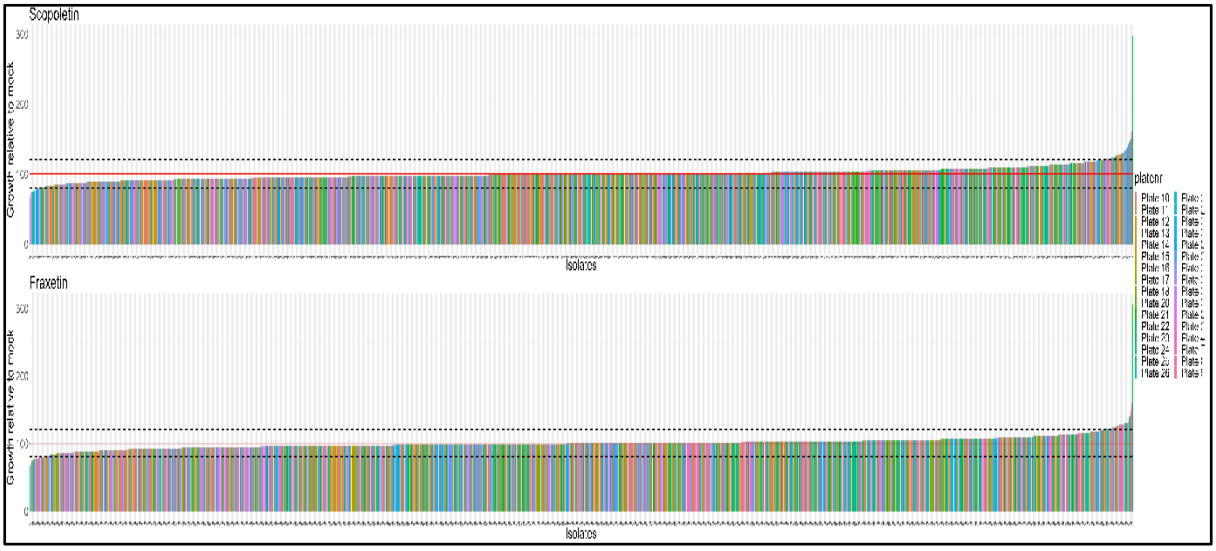

Figure S1: Preselection from the colony picking approach, previously performed by Chavan (Unpublished). *Candidates were isolated and tested for growth as measured by OD_{600} in 2 mM scopoletin (upper) or 0.75 mM fraxetin (lower). Shown is the growth relative to mock conditions, and isolates are ordered by relative growth, as well as colour coded for the microplate containing them.*

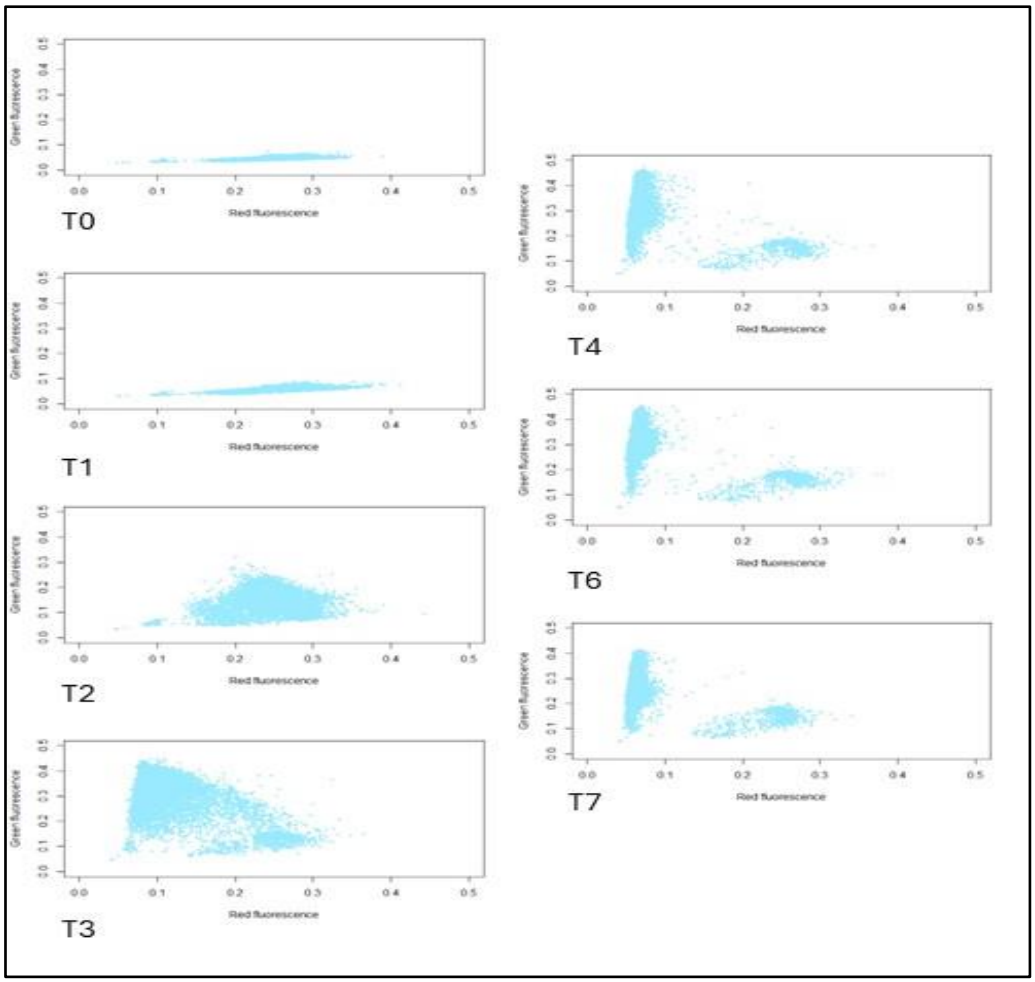

Figure S2: Red and green fluorescence in Prospector wells containing scopoletin over time. *Green fluorescence indicates growth. Here, wells with relatively slower growth were selected for further screening.*

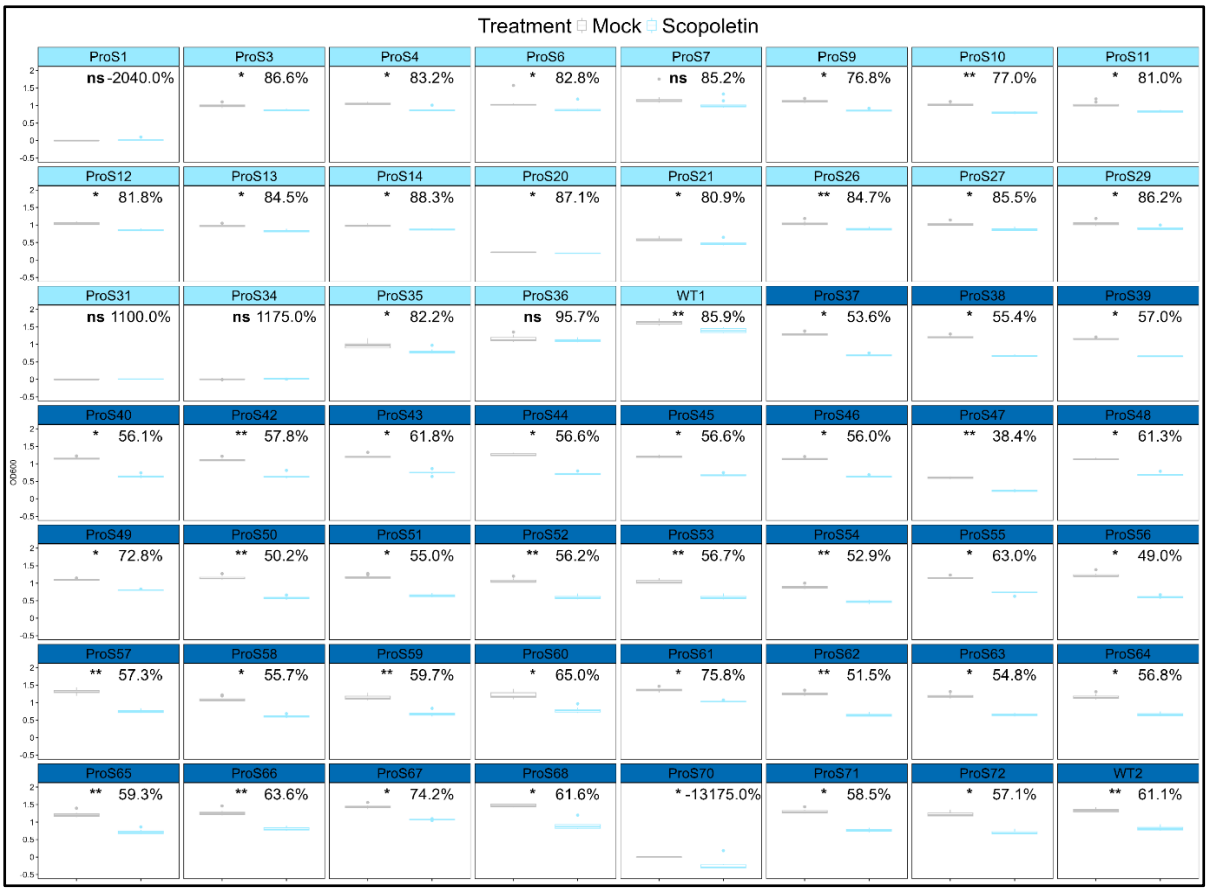

Figure S3: Candidates isolated using the Isolation Bio Prospector system tested for scopoletin tolerance in R2A medium. *Growth of candidates was tested in R2A medium with scopoletin and mock conditions, more similar to conditions of preselection in the Prospector system. Growth in scopoletin relative to mock conditions is shown. Significance level is indicated (ns, $p \geq 0.05$; *, $p < 0.05$; **, $p < 0.01$).*

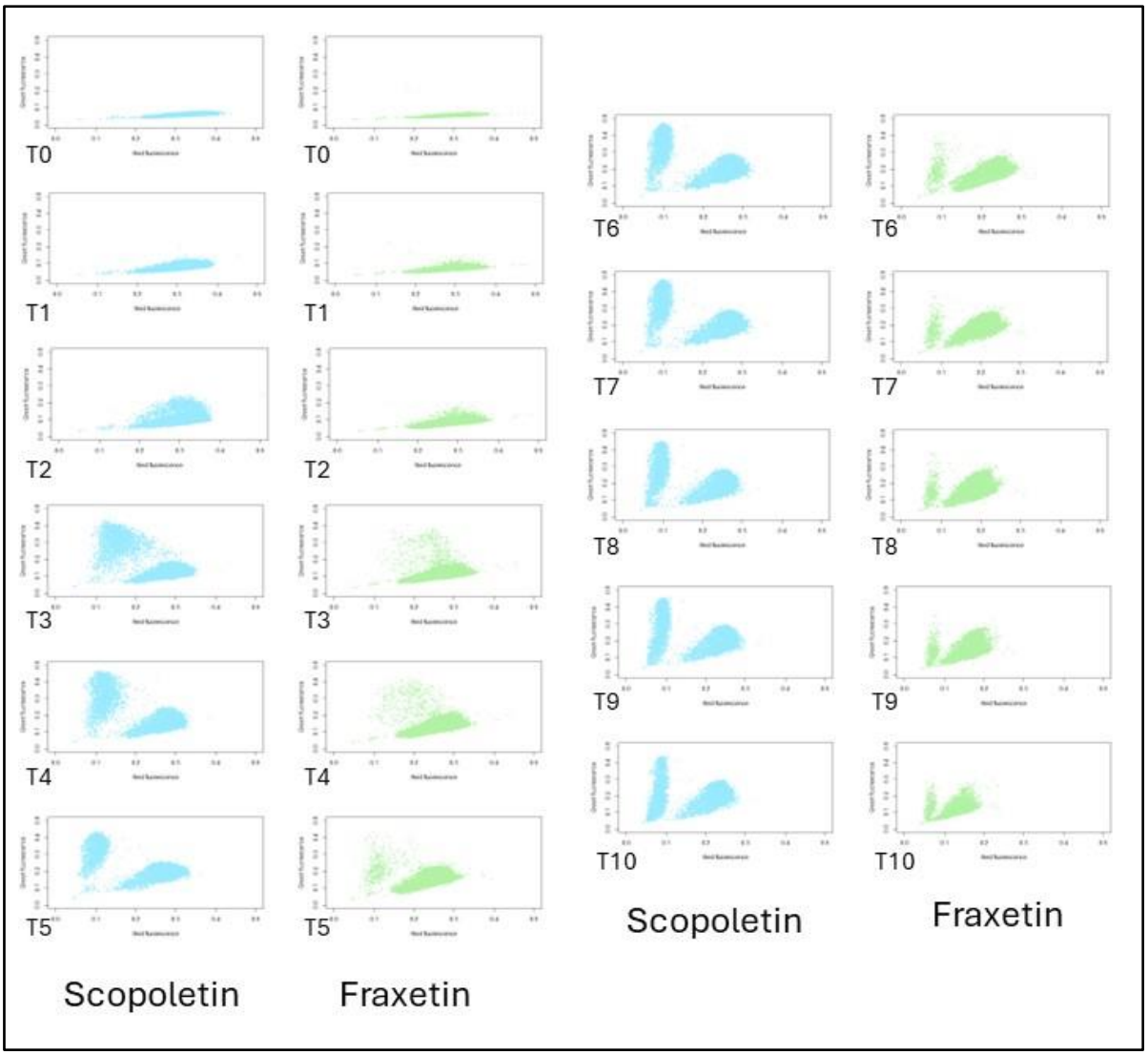

Figure S4: Red and green fluorescence in Prospector wells containing scopoletin and fraxetin over time. *Green fluorescence indicates growth. Here, wells with relatively slower growth were selected for further screening for both treatments.*

Figure S5: Candidates isolated using the Isolation Bio Prospector system tested for fraxetin tolerance in R2A medium. *Growth of candidates was tested in R2A medium with fraxetin and mock conditions, more similar to conditions of preselection in the Prospector system. Growth in scopoletin relative to mock conditions is shown. Significance level is indicated (ns, $p \geq 0.05$; *, $p < 0.05$).*

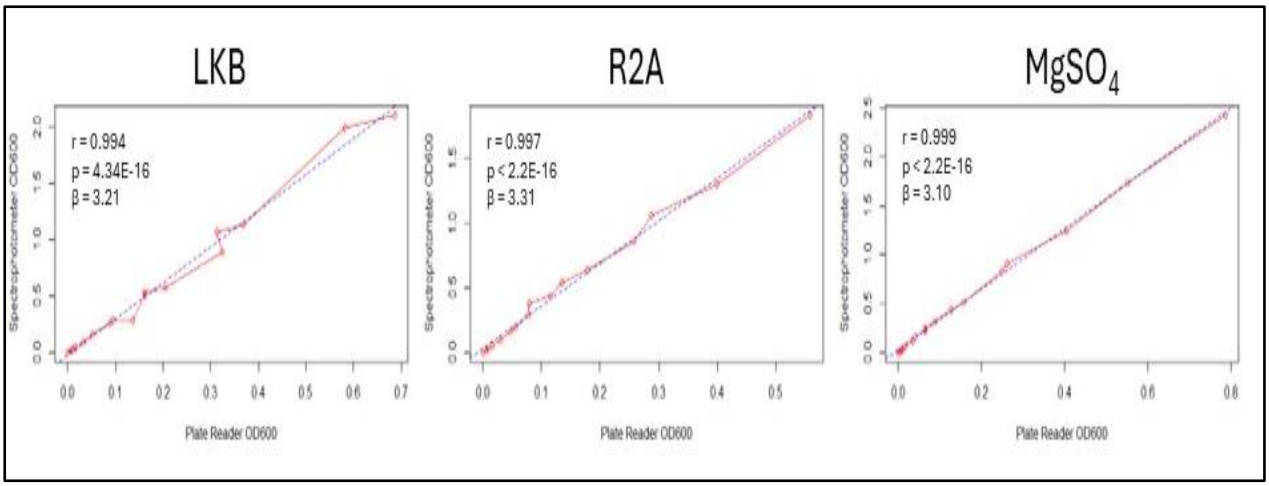

Figure S6: Results from pathlength correction experiments using spectrophotometer and a microplate reader. *The Pearson correlation coefficient, p-value and multiplication factor for pathlength correction (here β for the regression coefficient) of the microplate reader results are given for LKB, R2A, and* $MgSO_4$.

Figure S7: A representative example of plants grown in low-iron conditions. *17-day old* A. thaliana *Col-0 (A&B) and* s8h-1 *(C&D) plants growing on Hoagland medium mixed with* P. simiae *WCS417 wild type (A&C) or* pvd^- *(B&D).*

Figure S8: A representative example of plants grown in the double-layer agar system. *17-day old* A. thaliana *Col-0 (A&B) and* f6'h1 *(C&D) plants growing on 2 layers of Hoagland medium (not visible), the lower mixed with* P. simiae *WCS417 wild type (A&C) or* pvd$^-$ *(B&D), and the upper originally sterile.*